Fitoterapia 106 (2015) 147–152

Contents lists available at ScienceDirect

Fitoterapia

journal homepage: www.elsevier.com/locate/fitote

Salicin derivatives from *Salix glandulosa* and their biological activities

Chung Sub Kim [a], Lalita Subedi [b,c], Kyoung Jin Park [a], Sun Yeou Kim [b,c], Sang Un Choi [d], Ki Hyun Kim [a], Kang Ro Lee [a]

[a] Natural Products Laboratory, School of Pharmacy, Sungkyunkwan University, Suwon 440-746, Republic of Korea
[b] Gachon Institute of Pharmaceutical Science, Gachon University, Incheon, 406-799, Republic of Korea
[c] College of Pharmacy, Gachon University, #191, Hambakmoero, Yeonsu-gu, Incheon 406-799, Republic of Korea
[d] Korea Research Institute of Chemical Technology, Daejeon 305-600, Republic of Korea

ARTICLE INFO

Article history:
Received 18 June 2015
Received in revised form 26 August 2015
Accepted 28 August 2015
Available online 4 September 2015

Keywords:
Salix glandulosa
Salicaceae
Salicin derivatives
Nitric oxide
Nerve growth factor

ABSTRACT

Two new salicin derivatives, saliglandin (**1**) and 6′-O-(*Z*)-*p*-coumaroylsalicin (**2**), along with fourteen known analogues (**3**–**16**) were isolated from the twigs of *Salix glandulosa* Seemen. The structures of **1**–**16** were characterized by the use of NMR methods (^{1}H and ^{13}C NMR, ^{1}H-^{1}H COSY, HSQC and HMBC), chemical hydrolysis, and GC/MS. The full NMR data assignment of the known compounds **6**, **13**, and **14** are reported for the first time. Isolated compounds were evaluated for their nitric oxide (NO) inhibitory efficacy in lipopolysaccharide (LPS)-activated microglial cell (BV-2). Compounds **2**, **5**, **8**–**16** significantly inhibited NO production, compound **11** being the most efficacious (IC_{50} 13.57 μM) respectively. Moreover, compound **16** dramatically increased the nerve growth factor (NGF) production (165.24 ± 11.1%) in C6 glioma cells. Taken together, these results revealed that salicin derivatives from *Salix glandulosa* might have potent effect as anti-neuroinflammatory agents.

1. Introduction

Salix glandulosa Seemen (= *S. chaenomeloides* Kimura, Salicaceae), also known as “Korean King Willow”, is an indigenous plant in East Asia. The genus *Salix* is known as important medicinal herbs, since salicin, a precursor of acetylsalicylic acid (aspirin), flavonoids, terpenoids, lignans and phenolic compounds with biological activities have been reported from these sources [1–5]. Especially, salicin and salicylic acid have important pharmacological effects on treatment of fever, pain, and inflammation, whereas acetylsalicylic acid (aspirin), having similar activities, is a less toxic compound [6]. However, only few studies on phytochemical and biological investigations on *S. glandulosa* have been reported previously. The presence of several constituents, including salicin derivatives and flavonoids, were reported from *S. glandulosa* by Mizuo [7].

In our continuing search for biological constituents from Korean medicinal plants, we recently reported 13 phenolic glycosides correlated with anti-inflammatory activities from *S. glandulosa* [8]. In the process of finding new compounds from this plant, we further isolated two new salicin derivatives (**1** and **2**), along with 14 known ones (**3**–**16**) (Fig. 1). The chemical structures of new compounds were determined by NMR (^{1}H and ^{13}C NMR, ^{1}H-^{1}H COSY, HSQC, and HMBC), HRMS spectra, chemical hydrolysis, and GC/MS analysis. The isolated compounds (**1**–**16**) were evaluated for their anti-inflammatory, neuroprotective, and anticancer activities. Herein this paper we describe the isolation and structural elucidation of bioactive components from *S. glandulosa* and their biological activities.

2. Experimental

2.1. General experimental procedures

Optical rotations were measured on a JASCO P-1020 polarimeter. Infrared spectra were recorded on a Bruker IFS-66/S FT-IR spectrometer. UV spectra were recorded using an Agilent 8453 UV–visible spectrophotometer. NMR spectra were recorded on a Bruker AVANCE III 700 NMR spectrometer operating at 700 MHz (^{1}H) and 175 MHz (^{13}C). HRFABMS were obtained on a Waters SYNAPT G2 and JEOL JMS700 mass spectrometer. Silica gel 60 (Merck, 230–400 mesh) and RP-C_{18} silica gel (Merck, 230–400 mesh) was used for column chromatography (CC). Preparative HPLC was performed using a Gilson 306 pump with a Shodex refractive index detector. TLC was performed using Merck pre-coated Silica gel F_{254} plates and RP-18 F_{254s} plates.

2.2. Plant material

Twigs of *S. glandulosa* were collected from Gunwi, Korea in March 2013, and the plant was identified by one of the authors (K. R. L.). A voucher specimen (SKKU-NPL 1304) has been deposited in the herbarium of the School of Pharmacy, Sungkyunkwan University, Suwon, Korea.

2.3. Extraction and isolation

The dried twigs of *S. glandulosa* (10 kg) were extracted with 80% aq. MeOH under reflux. The MeOH extract was suspended with water and

http://dx.doi.org/10.1016/j.fitote.2015.08.013
0367-326X/

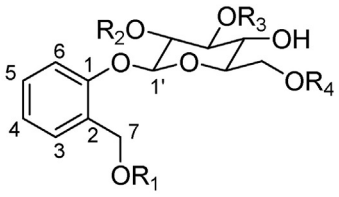

	R_1	R_2	R_3	R_4
1	X	Ac	H	H
2	H	H	H	(*Z*)-*p*-coumaroyl
3	H	H	H	H
4	H	Ac	H	H
5	H	H	Ac	H
6	H	H	H	Ac
7	H	benzoyl	H	H
8	H	(*E*)-*p*-coumaroyl	H	H
9	H	(*Z*)-*p*-coumaroyl	H	H
10	H	H	H	(*E*)-*p*-coumaroyl
11	Y	H	H	H
12	Y	Ac	H	H
13	Y	H	Ac	H
14	Y	H	H	Ac
15	Y	benzoyl	H	H
16	Y	H	benzoyl	H

X =

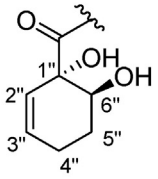

Y =

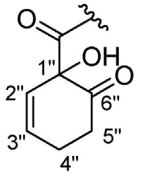

Fig. 1. Chemical structures of compounds **1–16**.

successively extracted with *n*-hexane (7 g), $CHCl_3$ (13 g), EtOAc (65 g) and *n*-butanol (100 g). The $CHCl_3$-soluble layer (13 g) was applied to a silica gel column ($CHCl_3$-MeOH, 20:1) to yeild 11 fractions (C1-C11). Fraction C4 (1.4 g) was separated on RP-C_{18} silica gel column (60% aq. MeOH) and further purified by semi-preparative HPLC (35% aq. CH_3CN) to yield compound **16** (3 mg). Fraction C7 (1.0 g) was subjected to a Sephadex LH-20 column (CH_2Cl_2-MeOH, 1:1) to yield three fractions (C7a-C7c). Fraction C7a (100 mg) and C7b (500 mg) were purified by semi-preparative HPLC (45% aq. CH_3CN) to give compounds **5** (9 mg), **13** (30 mg), and **14** (5 mg) from C7a, and **15** (200 mg) from C7b. Compound **12** (500 mg) was acquired from fraction C8 (1.8 g) by RP-C_{18} silica gel column (60% aq. MeOH) and semi-preparative HPLC (45% aq. CH_3CN). The EtOAc-soluble layer (20 g) was chromatographed over a silica gel column ($CHCl_3$-MeOH-H_2O, 4:1:0.1) to gave 11 fractions (E1-E11). Fraction E3 (2.5 g) was separated on a RP-C_{18} silica gel column with 50% aq. MeOH to yield seven subfractions (E3a-E3g). Fraction E3b (1.4 g) was applied to a silica gel column ($CHCl_3$-MeOH-H_2O, 6:1:0.05) and further purified by semi-preparative HPLC (20% aq. CH_3CN) to yield compounds **3** (10 mg), **4** (28 mg), **6** (11 mg), and **11** (10 mg). Fraction E3c (600 mg) was separated through a silica gel column ($CHCl_3$-MeOH-H_2O, 6:1:0.1) and further purified by semi-preparative HPLC (23% aq. CH_3CN) to yield compound **1** (6 mg). Compounds **8** (5 mg) and **9** (4 mg) were obtained from fraction E3d (90 mg) by semi-preparative HPLC (25% aq. CH_3CN). Fraction E3e (90 mg) was purified by semi-preparative HPLC (27% aq. CH_3CN) to give compounds **2** (2 mg), **7** (4 mg), and **10** (4 mg).

*2.3.1. Saliglandin (**1**)*

White powder; mp 181–182 °C; $[\alpha]_D^{25}$–47.1 (c 0.07, MeOH); IR (KBr) ν_{max} 3346, 2898, 1713, 1599, 1472 cm^{-1}; UV (MeOH) λ_{max} (log ε) 274 (1.31), 219 (4.00) nm; ^1H (CD_3OD, 700 MHz) and ^{13}C NMR (CD_3OD, 175 MHz) data, see Table 1; positive HRFABMS m/z 491.1529 $[M + Na]^+$ (calcd for $C_{22}H_{28}O_{11}Na$, 491.1529).

*2.3.2. 6′-O-(Z)-p-coumaroylsalicin (**2**)*

Colorless gum; $[\alpha]_D^{25}$ + 80.0 (c 0.02, MeOH); IR (KBr) ν_{max} 3344, 2901, 1715, 1601, 1466 cm^{-1}; UV (MeOH) λ_{max} (log ε) 305 (1.11), 271 (1.50), 220 (4.13) nm; ^1H (CD_3OD, 700 MHz) and ^{13}C NMR

Table 1
^1H (700 MHz) and ^{13}C (175 MHz) NMR data of compounds **1** and **2** in CD_3OD (700 MHz).

Pos.	1		2	
	δ_H (mult, *J* in Hz)	δ_C	δ_H (mult, *J* in Hz)	δ_C
1		156.2		157.1
2		127.0		132.4
3	7.42 (dd, 8.0, 1.5)	129.7	7.32 (dd, 7.7, 1.4)	130.0
4	7.06 (td, 8.0, 1.0)	124.0	7.01 (td, 7.7, 0.7)	124.0
5	7.30 (td, 8.0, 1.5)	130.4	7.19 (td, 7.7, 1.4)	130.1
6	7.23 (dd, 8.0, 1.0)	116.9	7.12 (brd, 7.7)	117.3
7a	5.21 (d, 13.4)	63.2	4.78 (d, 12.6)	61.2
7b	5.19 (d, 13.4)		4.57 (d, 12.6)	
1′	5.10 (d, 8.0)	100.9	4.83 (d, 7.7)	103.5
2′	5.04 (dd, 9.6, 8.0)	75.2	3.51 (dd, 8.4, 7.7)	75.2
3′	3.66 (t, 9.6)	76.1	3.46 (t, 8.4)	78.1
4′	3.51 (overlap)	74.8	3.39 (overlap)	71.8
5′	3.51 (overlap)	78.5	3.65 (ddd, 9.8, 6.3, 2.1)	75.7
6′a	3.94 (dd, 12.1, 1.5)	62.5	4.49 (dd, 11.9, 2.1)	64.5
6′b	3.76 (dd, 12.1, 6.0)		4.32 (dd, 11.9, 6.3)	
1″		78.1		127.7
2″	5.62 (dt, 10.0, 2.1)	127.8	7.62 (d, 8.4)	133.9
3″	5.96 (ddd, 10.0, 4.0, 3.2)	132.3	6.71 (d, 8.4)	116.0
4″a	2.29 (m)	24.4		160.3
4″b	2.19 (m)			
5″a	2.13 (m)	27.7	6.71 (d, 8.4)	116.0
5″b	1.93 (m)			
6″	3.90 (dd, 10.0, 3.8)	74.8	7.62 (d, 8.4)	133.9
7″		174.6	6.89 (d, 12.6)	145.6
8″			5.80 (d, 12.6)	116.3
9″				168.2
CH_3	2.16 (s)	21.3		
CO		172.2		

(CD_3OD, 175 MHz) data, see Table 1; positive HRFABMS m/z 433.1498 $[M + H]^+$ (calcd for $C_{22}H_{25}O_9$, 433.1499).

2.3.3. Fragilin (**6**)

White powder; mp 178–180 °C; $[\alpha]_D^{25}$–40.3 (c 0.10, MeOH); IR (KBr) ν_{max} 3330, 2900, 1715, 1611, 1477 cm^{-1}; UV (MeOH) λ_{max} (log ε) 272 (1.13), 219 (3.83) nm; ^1H (CD_3OD, 700 MHz) and ^{13}C NMR (CD_3OD, 175 MHz) data, see Table 2; positive HRFABMS m/z 351.1054 $[M + Na]^+$ (calcd for $C_{15}H_{20}O_8Na$, 351.1056).

2.3.4. 3′-O-acetylsalicortin (**13**)

White powder; mp 183–185 °C; $[\alpha]_D^{25}$–51.4 (c 0.30, MeOH); IR (KBr) ν_{max} 3350, 2910, 1710, 1611, 1458 cm^{-1}; UV (MeOH) λ_{max} (log ε) 270 (1.55), 219 (3.94) nm; ^1H (CD_3OD, 700 MHz) and ^{13}C NMR (CD_3OD, 175 MHz) data, see Table 2; positive HRFABMS m/z 489.1375 $[M + Na]^+$ (calcd for $C_{22}H_{26}O_{11}Na$, 489.1373).

2.3.5. 6′-O-acetylsalicortin (**14**)

White powder; mp 186–188 °C; $[\alpha]_D^{25}$–48.9 (c 0.30, MeOH); IR (KBr) ν_{max} 3355, 2911, 1711, 1608, 1460 cm^{-1}; UV (MeOH) λ_{max} (log ε) 270 (1.58), 220 (3.89) nm; ^1H (CD_3OD, 700 MHz) and ^{13}C NMR (CD_3OD, 175 MHz) data, see Table 2; positive HRFABMS m/z 489.1371 $[M + Na]^+$ (calcd for $C_{22}H_{26}O_{11}Na$, 489.1373).

Table 2
^1H (700 MHz) and ^{13}C (175 MHz) NMR data of compounds **6**, **13** and **14** in CD_3OD (700 MHz).

Pos.	6		13		14	
	δ_H (mult, *J* in Hz)	δ_C	δ_H (mult, *J* in Hz)	δ_C	δ_H (mult, *J* in Hz)	δ_C
1		157.1		157.0		157.0
2		130.0		126.4		126.6
3	7.37 (dd, 7.8, 1.6)	132.5	7.32 (dd, 7.5, 1.5)	130.8	7.32 (overlap)	131.0
4	7.07 (td, 7.8, 1.0)	124.0	7.06 (td, 7.5, 0.9)	123.8	7.06 (td, 7.5, 0.9)	123.8
5	7.28 (td, 7.8, 1.7)	130.0	7.35 (brt, 7.5)	131.2	7.34 (overlap)	131.1
6	7.17 (dd, 7.8, 1.0)	117.2	7.25 (brd, 7.5)	117.0	7.17 (brd, 7.5)	117.0
7a	4.80 (d, 13.0)	61.1	5.39 (d, 12.4)	64.5	5.39 (d, 12.4)	64.6
7b	4.60 (d, 13.0)		5.28 (d, 12.4)		5.28 (d, 12.4)	
1′	4.89 (d, 7.7)	103.4	5.05 (d, 7.8)	102.5	4.94 (d, 7.8)	102.6
2′	3.53 (dd, 9.2, 7.7)	75.1	3.63 (dd, 7.8, 9.4)	73.3	3.50 (overlap)	75.0
3′	3.49 (t, 9.2)	78.0	5.08 (t, 9.4)	79.1	3.50 (overlap)	78.0
4′	3.41 (dd, *J* = 9.6, 9.2)	71.7	3.60 (t, 9.6)	69.6	3.41 (t, 9.7)	71.7
5′	3.65 (ddd, *J* = 9.6, 6.4, 2.2)	75.6	3.55 (ddd, 9.9, 5.3, 2.2)	78.1	3.65 (ddd, 9.7, 6.5, 2.2)	75.5
6′a	4.43 (dd, 11.9, 2.2)	64.8	3.91 (dd, 12.1, 2.2)	62.3	4.40 (dd, 11.9, 2.2)	64.7
6′b	4.28 (dd, 11.9, 6.5)		3.75 (dd, 12.1, 5.3)		4.29 (dd, 11.9, 6.5)	
1″				79.3		79.4
2″			5.78 (dt, 9.8, 1.8)	129.4	5.78 (dt, 9.6, 1.8)	129.5
3″			6.17 (dt, 9.8, 4.0)	133.5	6.17 (dt, 9.6, 3.8)	133.5
4″a			2.67 (m)	27.4	2.67 (m)	27.4
4″b			2.53 (m)		2.53 (m)	
5″a			2.91 (m)	37.0	2.90 (m)	37.0
5″b			2.56 (m)		2.56 (m)	
6″				207.6		207.5
7″				171.6		171.6
8″						
9″						
CH_3	2.07 (s)	20.8	2.17 (s)	21.3	2.06 (s)	20.9
CO		172.8		172.8		172.8

2.4. Acid hydrolysis of 1 and 2 and sugar analysis

Compounds **1** and **2** (1.0 mg) were refluxed with 1 mL of 1 N HCl for 1 h at 90 °C. The hydrolysate was extracted with $CHCl_3$ and the aquatic layer was neutralized through an Amberlite IRA-67 column to give the sugar. The sugar obtained from the hydrolysis was dissolved in anhydrous pyridine (0.5 mL) followed by adding of 2.0 mg of L-cysteine methyl ester hydrochloride (Sigma). The mixture was stirred at 60 °C for 1.5 h and trimethylsilylated with 0.1 mL of 1-trimethylsilylimidazole (Sigma) for 2 h. The mixture was partitioned between *n*-hexane and H_2O (1.0 mL each), and the organic layer (1.0 μL) was analyzed by GC/MS [9]. Identification of D-glucose was detected by co-TLC ($CHCl_3$:MeOH:H_2O = 2:1:0.2, R_f value: 0.2) with a authentic sample, specific optical rotation {($[\alpha]_D^{25}$ + 60.1) (*c* 0.05, H_2O)}, and co-injection of the hydrolysate with standard silylated samples, giving a single peak at 9.855 min. Authentic samples (Sigma) treated in the same way showed a single peak at 9.860 min.

2.5. Preparation of Mosher ester derivatives **1r** and **1 s**

Compound **1** (0.5 mg) in deuterated pyridine (0.6 mL) was transferred into a clean NMR tube. (*S*)-(+)-α-Methoxy-α-(trifluoromethyl) phenylacetyl (MTPA) chloride (10 μL) (Sigma, St. Louis, MO) was added immediately into the NMR tube under a N_2 gas stream, and then the NMR tube was shaken carefully to mix the sample and MTPA chloride evenly. The NMR reaction tube was left at room temperature overnight. The reaction was then completed to afford the (*R*)-MTPA ester derivative (**1r**) of **1**. The (*S*)-MTPA ester derivative of **1** (**1s**) was obtained as described for **1r**. The ^1H NMR spectra of **1r** and **1s** were measured directly in the NMR reaction tubes.

2.5.1. 1-(R)-MTPA ester (**1r**)

^1H NMR (pyridine-d_5, 700 MHz) δ_H 6.18 (1 H, dt, *J* = 10.3, 2.2 Hz, H-2″), 5.99 (1 H, dt, *J* = 10.3, 3.7 Hz, H-3″), 5.94 (1 H, dd, *J* = 8.6, 3.1 Hz, H-6″), 6.02 (1 H, dd, *J* = 9.7, 8.0 Hz, H-2′), 5.94 (1 H, d, *J* = 8.0 Hz, H-1′), 5.87 (1 H, t, *J* = 9.7 Hz, H-4′), 5.72 (1 H, d, *J* = 12.8 Hz, H-7a), 5.63 (1 H, d, *J* = 12.8 Hz, H-7b), 4.90 (1 H, dd, *J* = 12.3, 1.7 Hz, H-6′a), 4.51 (1 H, t, *J* = 9.7 Hz, H-3′), 4.42 (1 H, ddd, *J* = 10.0, 5.2, 1.7 Hz, H-5′), 4.37 (1 H, dd, *J* = 12.3, 5.2 Hz, H-6′b), 2.48 (1 H, m, H-5″a), 2.30 (1 H, m, H-5″b), 2.21 (1 H, m, H-4″a), 2.12 (1 H, m, H-4″b); positive FABMS *m/z* 900.2 $[M + Na]^+$.

2.5.2. 1-(S)-MTPA ester (**1s**)

^1H NMR (pyridine-d_5, 700 MHz) δ_H 6.13 (1 H, dt, *J* = 10.3, 2.2 Hz, H-2″), 5.96 (1 H, dd, *J* = 9.8, 8.0 Hz, H-2′), 5.93 (1 H, d, *J* = 8.0 Hz, H-1′), 5.92 (2 H, overlap, H-3″ and H-6″), 5.83 (1 H, t, *J* = 9.7 Hz, H-4′), 5.79 (1 H, d, *J* = 12.6 Hz, H-7a), 5.73 (1 H, d, *J* = 12.6 Hz, H-7b), 5.00 (1 H, dd, *J* = 12.3, 1.6 Hz, H-6′a), 4.72 (1 H, dd, *J* = 12.3, 6.3 Hz, H-6′b), 4.52 (1 H, ddd, *J* = 10.0, 6.3, 1.6 Hz, H-5′), 4.50 (1 H, t, *J* = 9.7 Hz, H-3′), 2.38 (1 H, m, H-5″a), 2.23 (1 H, m, H-5″b), 2.06 (2 H, m, H-4″a and H-4″b); positive FABMS *m/z* 900.2 $[M + Na]^+$.

2.6. Cell cultures

Murine microglia BV2 was maintained in Dulbecco's Modified Eagle medium (DMEM), supplemented with 5% fetal bovine serum (Gibco), 100 units/mL penicillin, and 100 μg/mL streptomycin. All cells were incubated at 37 °C in a humidified incubator with 5% CO_2. All tumor cell cultures were maintained using RPMI1640 cell growth medium (Gibco, Carlsbad, CA), supplemented with 5% FBS, 100 units/mL penicillin, and 100 g/mL streptomycin.

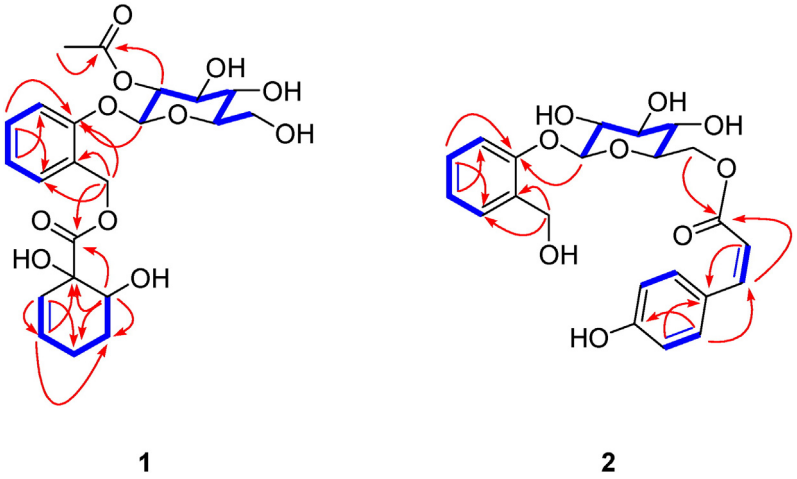

Fig. 2. Key HMBC and ^{1}H-^{1}H COSY correlations of **1** and **2**.

2.7. Measurement of nitric oxide production and cell viability

BV-2 cells were plated into a 96-well plate (3×10^4 cells/well). After 24 h, cells were pretreated with compounds **1** and **2** for 30 min, and then stimulated with 100 ng/ml of LPS for another 24 h. Nitrite, a soluble oxidation product of NO, was measured in the culture media using the Griess reaction. The supernatant was harvested and mixed with an equal volume of Griess reagent (1% sulfanilamide, 0.1% N-1-napthylethylenediamine dihydrochloride in 5% phosphoric acid). After 10 min, the absorbance at 570 nm was measured using a microplate reader. Sodium nitrite was used as a standard to calculate the NO_2^- concentration. Cell viability was assessed by a 3-[4, 5-dimethylthiazol-2-yl]-2, 5-diphenyl-tetrazolium bromide (MTT) assay. N^G-monomethyl-L-arginine (L-NMMA, Sigma, St. Louis, MO, USA), a well-known nitric oxide synthase (NOS) inhibitor, was tested as a positive control [10].

2.8. NGF and cell viability assays

C6 glioma cells were used to measure nerve growth factor (NGF) release into the medium. C6 cells were purchased from the Korean Cell Line Bank and maintained in DMEM supplemented with 10% FBS and 1% penicillin-streptomycin in a humidified incubator with 5% CO_2. To measure NGF content in the medium and cell viability, C6 cells were seeded into 24-well plates (1×10^5 cells/well). After 24 h, the cells were treated with DMEM containing 2% FBS and 1% penicillin-streptomycin with 20 μM of each sample for one day. Media supernatant was used for the NGF assay using an ELISA development kit (R&D Systems) [11]. Cell viability was assessed by the MTT assay.

3. Results and discussion

Compound 1 was isolated as a white powder (mp 181–182 °C) with the molecular formula of $C_{22}H_{28}O_{11}$ determined from the pseudomolecular ion peak $[M + Na]^+$ at *m/z* 491.1529 (calcd for $C_{22}H_{28}O_{11}Na$, 491.1529) in the HRFABMS. The IR spectrum of 1 showed absorption bands at 3346 and 1713 cm^{-1}, which were indicative of hydroxyl and carbonyl groups, respectively. The UV maxima at 274 and 219 nm indicated that 1 possessed aromatic ring. The ^{1}H NMR spectrum of 1 exhibited the presence of a 1,2-disubstituted aromatic ring [δ_H 7.42 (1 H, dd, J = 8.0, 1.5 Hz), 7.30 (1 H, td, J = 8.0, 1.5 Hz), 7.23 (1 H, dd, J = 8.0, 1.0 Hz), and 7.06 (1 H, td, J = 8.0, 1.0 Hz)], a *cis*-double bond [δ_H 5.96 (1 H, ddd, J = 10.0, 4.0, 3.2 Hz) and 5.62 (1 H, dt, J = 10.0, 2.1 Hz)], an oxygenated methylene [δ_H 5.21 (1 H, d, J = 13.4 Hz) and 5.19 (1 H, d, J = 13.4 Hz)], a sugar unit [δ_H 5.10 (1 H, d, J = 8.0 Hz), 5.04 (1 H, dd, J = 9.6, 8.0 Hz), 3.94 (1 H, dd, J = 12.1, 1.5 Hz), 3.76 (1 H, dd, J = 12.1, 6.0 Hz), 3.66 (1 H, t, J = 9.6 Hz), and 3.51 (2 H, overlap)], an oxygenated methine [δ_H 3.90 (1 H, dd, J = 10.0, 3.8 Hz)], two methylenes [δ_H 2.29 and 2.19 (each 1 H, m), and 2.13 and 1.93 (each 1 H, m)], and a methyl group [δ_H 2.16 (3 H, s)]. The ^{13}C NMR spectrum of 1 showed 22 carbon signals including two carbonyl carbon (δ_C 174.6 and 172.2), eight olefinic or aromatic carbon (δ_C 156.2, 132.3, 130.4, 129.7, 127.8, 127.0, 124.0, and 116.9), an acetalic carbon (δ_C 100.9), and eight oxygenated carbon [δ_C 78.5, 78.1, 76.1, 75.2, 74.8 (×2), 63.2, and 62.5] signals. These ^{1}H and ^{13}C NMR data of 1 implied that compound 1 may be a salicin derivative by the aforementioned evidence and reported literatures [3,7,12], and were very similar to tremulacinol [12], except for the signals attributable to an acetyl group at δ_H 2.16 (3 H, s) and δ_C 172.2 and 21.3, instead of benzoyl group present in tremulacinol. The HMBC correlation between H-2′ [δ_H 5.04 (1 H, dd, J = 9.6, 8.0 Hz)] and carbonyl carbon (δ_C 172.2) confirmed the location of acetyl group at C-2′. The gross structure of 1 was established by analysis of the ^{1}H-^{1}H COSY, HMQC, and HMBC spectra (Fig. 2). Acid hydrolysis of 1 yielded D-glucose, which was identified by co-TLC with authentic sample, specific optical rotation {($[\alpha]_D^{25}$ + 60.1) (*c* 0.05, H_2O)}, and GC/MS analysis. The relative configuration of hydroxyl groups at C-1″ and C-6″ in 1 was confirmed by comparing their ^{1}H and ^{13}C NMR data of 1 with those of related compounds. The chemical shifts of H-5″ [δ_H 2.13 and 1.93 (each 1 H, m)] were in ccordance with those of tremulacinol [δ_H 2.21–2.10 and 1.89–1.85 (each 1 H, m)] possessing *trans*-diol at C-1″ and C-6″ rather than its 6″-epimer [δ_H 1.76–1.73 (2 H, m)] with *cis*-diol at C-1″ and C-6″ [12]. In addition, the downfield shifted signals of C-1″ and C-6″ (δ_C 78.1

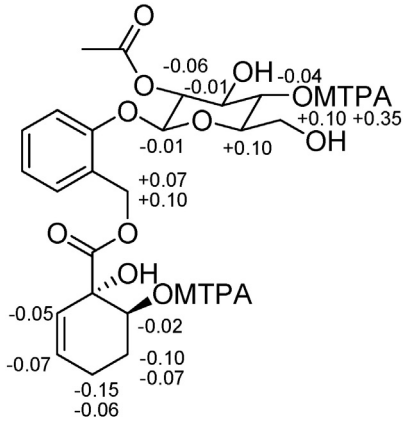

Fig. 3. Δδ values ($\delta_S - \delta_R$) in ppm of the two MTPA esters derived from **1**.

Table 3
Effects of compounds **1–16** and L-NMMA on LPS-induced NO production in BV-2 microglia cells.

Comp.	IC_{50} (μM)[a]	Cell viability (%)[b]	Comp.	IC_{50} (μM)[a]	Cell viability (%)[b]
1	120.18	113.74 ± 3.4	**10**	38.25	110.65 ± 6.9
2	31.55	95.75 ± 6.9	**11**	13.57	116.72 ± 4.7
3	85.40	112.68 ± 3.5	**12**	14.61	90.13 ± 7.7
4	123.36	105.97 ± 2.2	**13**	18.27	97.08 ± 10.8
5	27.27	91.98 ± 2.9	**14**	22.78	88.96 ± 7.9
6	206.12	106.79 ± 5.7	**15**	18.59	105.21 ± 3.8
7	114.30	110.06 ± 3.3	**16**	23.40	98.43 ± 10.7
8	29.77	119.59 ± 7.0	L-NMMA[c]	24.78	106.46 ± 5.0
9	25.47	112.25 ± 5.2			

[a] The IC_{50} value of each compound was defined as the concentration (μM) that caused 50% inhibition of NO production in LPS-activated BV-2 cells.
[b] Cell viability after treatment with 20 μM of each compound was determined by MTT assay and is expressed as a percentage (%). Results are means of three independent experiments, and the data are expressed as mean ± SD.
[c] L-NMMA as a positive control.

and 74.8, respectively) in 1 supported the relative configuration at C-1′′ and C-6′′ to be *trans* [δ_C 77.7 and 74.5, tremulacinol (*trans*-diol); δ_C 74.2 and 70.8, 6′′-epimer of tremulacinol (*cis*-diol)] [12]. The absolute configuration of C-6′′ was established on the basis of the modified Mosher's mothod [13,14]. Treatment of 1 with (*R*)- and (*S*)-MTPA-Cl gave the (*S*)- and (*R*)-MTPA esters 1s and 1r, respectively. The ^{1}H NMR signals of the two MTPA esters were assigned on the basis of their ^{1}H-^{1}H COSY spectra, and the $\Delta\delta$ values ($\delta_S - \delta_R$) were then calculated (Fig. 3). The results showed that the absolute configuration of C-6′′ was *S* form. Therefore, the structure of 1 was determined as shown in Fig. 1, and named saliglandin.

Compound **2** was obtained as a colorless gum. The HRFABMS data (*m/z* 433.1498 $[M + H]^+$, calcd for $C_{22}H_{25}O_9$, 433.1499) of **2** indicated that this molecule possessed the molecular formula $C_{22}H_{24}O_9$ with 11 degree of unsaturation. The ^{1}H and ^{13}C NMR data of **2** were quite similar to those of **10** [15] except for the chemical shifts of H-7′′ and H-8′′. The small *J* value (12.6 Hz) between H-7′′ and H-8′′ were indicative of *cis*-configuration. The ^{1}H and ^{13}C NMR signals of C-6′ in **2** [δ_H 4.49 (1 H, dd, J = 11.9, 2.1 Hz) and 4.32 (1 H, dd, J = 11.9, 6.3 Hz); δ_C 64.5] were downfield shifted compared with those in **3** [δ_H 3.92 (1 H, dd, J = 12.1, 2.0 Hz) and 3.73 (1 H, dd, J = 12.1, 6.2 Hz); δ_C 62.7], suggesting the location of (*Z*)-*p*-coumaroyl unit to be at C-6′. This was corroborated by the HMBC cross-peak between H-6′ and C-9′′ (δ_C 168.2).

Compounds **6** (fragilin), **13** (3′-*O*-acetylsalicortin), and **14** (6′-*O*-acetylsalicortin) are known ones reported previously, but their NMR data have not been reported [3,16,17]. We performed full NMR data assignments of **6**, **13**, and **14** through analysis of ^{1}H and ^{13}C NMR, ^{1}H-^{1}H COSY, HSQC, and HMBC spectra. To the best of our knowledge, the NMR data of **6**, **13**, and **14** are reported for the first time in this study.

The other known compounds were identified as salicin (**3**) [18], 2′-*O*-acetylsalicin (**4**) [19], 3′-*O*-acetylsalicin (**5**) [3], trumuloidin (**7**) [12], 2′-*O*-(*E*)-*p*-coumaroylsalicin (**8**) [17], 2′-*O*-(*Z*)-*p*-coumaroylsalicin (**9**) [17], 6′-O-(*E*)-*p*-coumaroylsalicin (**10**) [15], salicortin (**11**) [20], 2′-*O*-acetylsalicortin (**12**) [19], tremulacin (**15**) [12], and cochinchiside A (**16**) [12] by comparing their spectroscopic data with the values reported in the references.

All the isolates (**1–16**) were evaluated for their anti-inflammatory activities measuring nitric oxide (NO) production in lipopolysaccharide (LPS)-activated BV-2 cells, a microglial cell line. Among them, compounds **11–16** showed significant inhibition of NO production with IC_{50} values of 13.57, 14.61, 18.27, 22.78, 18.59, and 23.40 μM, respectively (Table 3), which displayed more activity than a positive control, L-NMMA (IC_{50} 24.78 μM). Interestingly, these compounds shared (1-hydroxy-6-oxocyclohex-2-en-1-yl)carboxylate substructure at C-7, which implies that (1-hydroxy-6-oxocyclohex-2-en-1-yl)carboxylate substructure may exert their NO inhibitory activity in salicin derivatives. Compounds **2** and **8–10** possessing *p*-coumaroyl moiety at glucosyl unit also exhibited potent activities with IC_{50} values of 31.55, 29.77, 25.47, and 38.25 μM, respectively. In addition, although the structures of **4–6** are very similar except for the location of acetyl group, only compound **5** showed potent inhibitory effect on NO production (IC_{50} 27.27 μM). These obtained data suggest that the location of the acetyl group at C-3′ in salicin derivatives may play a role for their NO inhibitory activity though more salicin derivatives need to be evaluated to confirm this hypothesis. There were no cytotoxic effects of all these compounds, as assessed by cell viabilty assay, at concentrations up to 20 μM.

Neuroprotection is possible through increased production of neurotrophins like NGF in neuronal environment. Compounds that can induce the production on NGF can be the effective neuroprotective agents against LPS induced neuronal death [21]. To investigate the effect of compounds **1–16** on neurotrophins, firstly, we measured secretion of NGF from C6 glioma cells into the medium. As shown in Table 4, compound **16** was significant stimulant of NGF release (165.24 ± 11.1%; 6-shogaol, a positive control, 141.75 ± 9.4%) without cell toxicity at concentration of 20 μM. Interestingly, the structure of compound **15** was quite similar to that of **16** except for the location of benzoyl group at C-2′, but compound **15** was inactive (64.58 ± 0.4%). This data suggest that benzoyl group at C-3′ may be very important for the secretion of NGF from C6 cells. In addition, compounds **2** and **10** possessing *p*-coumaroyl moiety at C-6′ exhibited mild induction of NGF secretion by 125.23 ± 7.0% and 124.68 ± 4.0%, respectively, whereas compounds **8** and **9** possessing *p*-coumaroyl moiety at C-2′ showed weak activity (91.06 ± 6.2% and 73.37 ± 1.3%, respectively).

Table 4
Effects of compounds **1–16** on NGF secretion in C6 cells.

Comp.	NGF secretion (%)[a]	Cell viability (%)[b]	Comp.	NGF secretion (%)[a]	Cell viability (%)[b]
1	105.21 ± 1.1	90.89 ± 0.6	**10**	124.68 ± 4.0	95.74 ± 0.6
2	125.23 ± 7.0	99.40 ± 0.5	**11**	124.71 ± 1.0	95.52 ± 0.4
3	99.44 ± 1.8	89.59 ± 0.3	**12**	33.77 ± 0.6	90.49 ± 1.3
4	102.87 ± 1.8	88.63 ± 0.6	**13**	91.91 ± 6.5	101.74 ± 0.2
5	77.47 ± 8.5	93.21 ± 0.5	**14**	21.46 ± 1.2	88.64 ± 0.7
6	84.78 ± 9.8	104.79 ± 5.2	**15**	64.58 ± 0.4	92.98 ± 1.2
7	88.27 ± 8.7	91.33 ± 0.5	**16**	165.24 ± 11.1	99.25 ± 2.5
8	91.06 ± 6.2	100.74 ± 1.0	6-Shogaol[c]	141.75 ± 9.4	105.83 ± 9.5
9	73.37 ± 1.3	100.71 ± 0.8			

[a] C6 cells were treated with 20 μM of the compounds. After 24 h, the content of NGF secreted in C6-conditioned media was measured by ELISA. The level of secreted NGF/cell is expressed as percentage of the untreated control. Data are means ± SD of three independent experiments performed in triplicate.
[b] Cell viability after treatment with 20 μM of each compound was determined by MTT assay and is expressed as a percentage (%). Results are means of three independent experiments, and the data are expressed as mean ± SD.
[c] 6- Shogaol as a positive control.

Conflict of interest

The authors indicated no potential conflicts of interest.

Acknowledgements

This research was supported by the Basic Science Research Program through the National Research Foundation of Korea (NRF) funded by the Ministry of Education, Science and Technology (2012R1A5A2A28671860). We are thankful to the Korea Basic Science Institute (KBSI) for the measurements of MS spectra.

Appendix A. Supplementary data

Supplementary data to this article can be found online at http://dx.doi.org/10.1016/j.fitote.2015.08.013.

References

[1] T.P. Evans, T.P. Clausen, P.B. Reichardt, Structurally intriguing glucosides from Alaskan littletree willow (*Salix arbusculoides*), J. Nat. Prod. 58 (1995) 1897–1900.

[2] F.-L. Hsu, G.-I. Nonaka, I. Nishioka, Acylated flavanols and procyanidins from *Salix sieboldiana*, Phytochemistry 24 (1985) 2089–2092.

[3] H. Yang, S.H. Lee, S.H. Sung, J. Kim, Y.C. Kim, Neuroprotective compounds from *Salix pseudo-lasiogyne* twigs and their anti-amnesic effects on scopolamine-induced memory deficit in mice, Planta Med. 78 (2013) 78–82.

[4] M.A. Tantry, S. Shah, M.Y. Dar, M.M. Mir, K. Ghazanfar, F.A. Sheikh, M.A. Khuroo, S. Akbar, 9,10-*seco*-9,19-cyclolanostane triterpene from *Salix caprea* L. (goat willow), Nat. Prod. Res. 27 (2013) 171–175.

[5] S.H. Jeon, W. Chun, Y.J. Choi, Y.S. Kwon, Cytotoxic constituents from the bark of *Salix hulteni*, Arch. Pharm. Res. 31 (2008) 978–982.

[6] R.K. Madan, J. Levitt, A review of toxicity from topical salicylic acid preparations, J. Am. Acad. Dermatol. 70 (2014) 788–792.

[7] M. Mizuno, M. Kato, C. Misu, M. Iinuma, T. Tanaka, Chaenomeloidin: a phenolic glucoside from leaves of *Salix chaenomeloides*, J. Nat. Prod. 54 (1991) 1447–1450.

[8] C.S. Kim, O.W. Kwon, S.Y. Kim, S.U. Choi, J.Y. Kim, J.Y. Han, S.I. Choi, J.G. Choi, K.H. Kim, K.R. Lee, Phenolic glycosides from the twigs of *Salix glandulosa*, J. Nat. Prod. 77 (2014) 1955–1961.

[9] C.S. Kim, O.W. Kwon, S.Y. Kim, K.H. Kim, K.R. Lee, A new cyclic triterpene saponin from *Phyteuma japonicum*, Heterocycles 89 (2014) 1913–1922.

[10] D.W. Reif, S.A. McCreedy, *N*-nitro-L-arginine and *N*-monomethyl-L-arginine exhibit a different pattern of inactivation toward the three nitric oxide synthases, Arch. Biochem. Biophys. 320 (1995) 170–176.

[11] J.P. Schwartz, E. Costa, Regulation of nerve growth factor content in C6 glioma cells by beta-adrenergic receptor stimulation, Naunyn Schmiedeberg's Arch. Pharmacol. 300 (1977) 123–129.

[12] T. Ishikawa, K. Nishigaya, K. Takami, H. Uchikoshi, I.-S. Chen, I.-L. Tsai, Isolation of salicin derivatives from *Homalium cochinchinensis* and their antiviral activities, J. Nat. Prod. 67 (2004) 659–663.

[13] K.H. Kim, S.U. Choi, Y.C. Kim, K.R. Lee, Tirucallane triterpenoids from *Cornus walteri*, J. Nat. Prod. 74 (2011) 54–59.

[14] C.S. Kim, S.Y. Kim, E. Moon, M.K. Lee, K.R. Lee, Steroidal constituents from the leaves of *Hosta longipes* and their inhibitory effects on nitric oxide production, Bioorg. Med. Chem. Lett. 23 (2013) 1771–1775.

[15] C.C. Fernandes, L.M.d.C. Cursino, J.d.A.P. Novaes, C.A. Demetrio, O.L. Pereira Jr., C.V. Nunez, I. Leao do Amaral, Salicylates isolated from leaves and stems of *Salix martiana* Leyb. (Salicaceae), Quim. Nova 32 (2009) 983–986.

[16] H. Thieme, Isolation of a new phenol glucoside from *Salix fragilis*, Naturwissenschaften 50 (1963) 477.

[17] E. Dagvadorj, K.H. Shaker, D. Windsor, B. Schneider, W. Boland, Phenolic glucosides from *Hasseltia floribunda*, Phytochemistry 71 (2010) 1900–1907.

[18] A. Itoh, T. Tanahashi, S. Ikejima, M. Inoue, N. Nagakura, K. Inoue, H. Kuwajima, H.-X. Wu, Five phenolic glycosides from *Alangium chinense*, J. Nat. Prod. 63 (2000) 95–98.

[19] P.B. Reichardt, H.M. Merken, T.P. Clausen, J. Wu, Phenolic glycosides from *Salix lasiandra*, J. Nat. Prod. 55 (1992) 970–973.

[20] R.A. Dommisse, L. Van Hoof, A.J. Vlietinck, Structural analysis of phenolic glucosides from Salicaceae by NMR spectroscopy, Phytochemistry 25 (1986) 1201–1204.

[21] R. Tabakman, H. Jiang, I. Shahar, H. Arien-Zakay, R.A. Levine, P. Lazarovici, Neuroprotection by NGF in the PC12 in vitro OGD model: involvement of mitogen-activated protein kinases and gene expression, Ann. N. Y. Acad. Sci. 1053 (2005) 84–96.